Biochemical Pharmacology, Vol. 52, pp. 49–63, 1996.

ISSN 0006-2952/96/$15.00 + 0.00
PII S0006-2952(96)00138-4

Simultaneous Measurement of Ca^{2+} Transients and Changes in the Cell Volume and Microviscosity of the Plasma Membrane in Smooth Muscle Cells

EVALUATION OF THE EFFECT OF FORMOTEROL

*Martin Ochsner**

CIBA-GEIGY LTD., DEPARTMENT OF PHYSICS, BASLE, SWITZERLAND

ABSTRACT. The effects of the β_2-adrenoceptor agonist formoterol (50 nM) on the angiotensin II (20 nM)-induced Ca^{2+} response and changes in the cell volume and microviscosity of the plasma membrane of vascular smooth muscle cells were studied. Applied as a model substance for the stimulation of the phosphoinositide-phospholipase C pathway, angiotensin II has been used to simulate the bronchospasm of smooth muscle in asthma. Our results demonstrated that angiotensin II-induced smooth muscle contraction primarily involves an $InsP_3$-mediated release of Ca^{2+} from intracellular stores and, to a minor extent, an enhanced influx of Ca^{2+} through the plasma membrane. Both the Ca^{2+} response and the contractile reaction were strongly antagonized by pretreatment of the cells with 50 nM formoterol. The protective effect of formoterol on smooth muscle contractions is proposed to be mainly related to a direct stimulation of β_2-adrenoceptor-coupled cAMP generation. Moreover, it is predicted that the interaction between the β_2-adrenoceptor glycoprotein and adenylate cyclase will be enhanced following a formoterol-associated decrease in the microviscosity of the plasma membrane. BIOCHEM PHARMACOL 52;1:49–63, 1996., 1996.

KEY WORDS. β_2-adrenoceptor agonist; formoterol; cAMP; Ca^{2+} transient; microviscosity of plasma membrane; contraction of smooth muscle cells

Contraction of airway smooth muscle is largely responsible for the bronchospasm that is one of the characteristic features of an asthmatic attack [1]. Neural bronchoconstrictor activity is mediated through the cholinergic section of the autonomic nervous system. Vagal sensory endings in airway epithelium initiate the afferent limb of a reflex arc, which stimulates smooth muscle contraction at the efferent end [2]. The condition of asthma may be acute or chronic and the attacks may vary widely in frequency and severity. A decreased number of β_2-adrenergic receptors (downregulation) on airway smooth muscle and inflammatory cells in asthmatic patients frequently leads to a reduced sensitivity of bronchial smooth muscle to endogenous or exogenous β_2-stimulatory catecholamines [2]. Shedding of the epithelium (desquamation) may cause a complete detachment of the mucosal and mucus-secreting cells, leaving only the lowest cell layer of the basement membrane intact [3]. Epithelial shedding is associated with an increase in intracellular space, and has been correlated with bronchial hyperreactivity because the loss of the bronchial epithelium denudes nerves and mast cells [3]. It is, therefore, not astonishing that airway smooth muscle cells of asthmatic patients are mostly hyperresponsive to a wide variety of provoking stimuli [4]. The pathological processes underlying asthmatic disease are inflammatory in nature, with a concurrent involvement of various mediators such as histamine, prostaglandins, hydroxyeicosatetraenoic acid, and the sulfido-peptide leukotrienes (LTC_4, LTD_4, and LTE_4) [5]. Inflammatory reactions are characterized by mucosal and bronchial wall edema, lymphocyte and eosinophil filtration, and the occurrence of mucus plugs within the airway lumen [4]. Due to the inflammatory character of the disease, the current approach in asthma therapy has, therefore, shifted away from bronchodilatory drugs [6–8]. International guidelines recommend inhaled corticosteroids or nonsteroidal anti-inflammatory drugs, such as cromolyn sodium and nedocromil sodium, as first-line therapy for the management of asthma [9, 10]. Nevertheless, there are still sufficient unanswered questions concerning long-term therapy with inhaled steroids that such treatment should be reserved for adults or children with severe asthma [11]. The prescription of bronchodilatory β_2-adrenoceptor agonists has been the main therapeutic approach for many years, especially for handling acute asthmatic attacks. Agents selective for β_2-adrenoceptors are preferentially delivered by inhalation and provide rapid and effective reversal of acute

* Corresponding author: Martin Ochsner, %Ciba-Geigy Ltd., Department of Physics, Im Kugelfang 40, CH-4102 Binningen, Switzerland.
Received 8 June 1995; accepted 23 January 1996.

airway obstructions, without causing severe cardiovascular side effects [4, 6].

Two new long-acting selective β_2-adrenoceptor agonists, formoterol and salmeterol, have recently become available for the treatment of airflow obstruction in asthma [12, 13]. Important differences have been observed *in vitro:* formoterol has a higher intrinsic efficacy and a faster onset of relaxation (1–3 minutes) than salmeterol [12, 13]. Following an inhalation of formoterol 12 μg [14] or salmeterol 50 μg [15], bronchodilatation is maintained for a minimum of 12 hr and protection afforded by both drugs against histamine and methacholine challenge is provided for up to 24 hr. Based on the estimates of Anderson *et al.*, a single inhalation of formoterol or salmeterol instantaneously leads to topical concentrations of at least 1 μM in the main bronchi [12, 13]. This represents a substantial bulk concentration that moves efficiently across the epithelium towards airway smooth muscle. Sufficient drug should, therefore, be available to allow an immediate interaction with the active site of the β_2-adrenoceptor glycoprotein. The model explains the rapid bronchodilatation observed after inhalation of formoterol, which has a threshold concentration for relaxation of human airway smooth muscle of less than 0.10 nM [12]. In contrast, bronchodilatation is delayed with salmeterol, the maximal therapeutic response being achieved up to 11 hr after administration of the drug [12, 13]. This slow onset of action is still a matter of scientific discussion and may be related to the higher lipophilicity of salmeterol [12, 13].

Recently, several research articles have been published suggesting a causal relationship between death from asthma and inhalation therapy with long-acting β_2-adrenoceptor agonists [16]. However, many experts reject the view that the use of β_2-receptor agonists, one of the cornerstones of asthma treatment, is potentially dangerous [17]. They argue that these drugs have preferentially been used for patients with a poor prognosis, thereby making it difficult to draw significant conclusions [18].

For the management of asthma, selective β_2-adrenoceptor agonists, such as salbutamol, formoterol, and salmeterol, are still widely used therapeutic agents. In this paper, the effects of formoterol (50 nM) on the angiotensin II (20 nM)-induced Ca^{2+} response and changes in the cell volume and microviscosity of the plasma membrane of vascular smooth muscle cells have been studied.

To establish a direct correlation between cytosolic Ca^{2+} concentration and the cell volume [19, 20] and microviscosity of the plasma membrane, an apparatus capable of measuring all 3 biological parameters simultaneously has been developed. Due to the discontinuous measurement techniques used, it has until now been impossible to gain an insight into the sequence and dynamic nature of the processes involved.

MATERIALS AND METHODS

Chemicals

Formoterol, an exact 1:1 mixture of the (R;R) and (S;S) enantiomers of (±)-(R*;R*)-(N-[2-hydroxy-5-[1-hydroxy-2-[[2-(p-methoxyphenyl)-2-propyl]amino]ethyl]phenyl] formamide formulated as fumarate dihydrate salt, was synthesized at Ciba-Geigy Ltd. (Basle, Switzerland). Trypsin buffer solution (0.25%) and tissue culture flasks were obtained from Gibco BRL (Basle, Switzerland); RPMI 1640 medium, penicillin, and streptomycin sulfate from Boehringer Mannheim (FRG); angiotensin II and ionomycin from Calbiochem (Lucerne, Switzerland); 1,6-diphenyl-1,3,5-hexatriene (DPH), fluo-3:AM, and 3,3′-diethylthiacarbocyanine iodide ($DiSC_2(3)$) from Molecular Probes (Eugene, OR, U.S.A.). All other chemical were from Fluka (Buchs, Switzerland).

Cell Culture

Primary cultures of vascular smooth muscle cells isolated from rat aorta were kindly provided by Prof. J. Pfeilschifter (Biocentre, University of Basle, Switzerland). Grown in an RPMI 1640 medium supplemented with 10% fetal calf serum, penicillin (100 U/mL), streptomycin sulfate (100 μg/mL), and bovine insulin (0.66 U/mL), vascular smooth muscle cells were cultivated in 75 cm^2 tissue culture flasks at 37°C in air/CO_2 (19:1) essentially as described previously [21, 22]. The cells were subcultured every 5–6 days and the culture media renewed every 2–3 days. Prior to starting the measurements, the cells ($3 \cdot 10^5/cm^2$) were harvested using the trypsin (0.25%) buffer solution, centrifuged (70 *g*; 5 min; 25°C) and suspended in RPMI 1640 medium at a density of 10^7 cells/mL. Viability was assessed thereafter by the Trypan Blue exclusion method, which indicated a survival rate of 96 (±1)%. Because vascular smooth muscle cells lose their ability to isotonically contract after multiple passages in culture, only early cell passages (No. 7–9) were used throughout the study. Finally, each cell line was extensively characterized using the following criteria: morphological analysis by phase-contrast light microscopy; positive staining for the characteristic cytoskeletal filaments of myogenic cells (i.e., actin, myosin, desmin and vimentin) [23, 24]; negative staining for factor VIII-related antigen and cytokeratin, excluding endothelial and epithelial contaminations [24], respectively; and contraction in response to angiotensin II (20 nM).

Measurement of Ca^{2+} Transients

To investigate changes in cytosolic $[Ca^{2+}]_i$ on a subsecond time-scale, a whole family of Ca^{2+} sensitive fluorescence indicators has been synthesized. Compared to the first and widely used representative quin-2, newly released indicators (indo-1, fura-2, and fluo-3) possess improved selectivity for Ca^{2+} and better spectroscopic qualities (i.e., brighter fluorescence and higher photostability) [25–27]. All our fluorescence assays were based on the spectroscopic determination of free and Ca^{2+}-bound fluo-3 concentration. Upon complexation of Ca^{2+}, the fluorescence intensity of fluo-3 increases by a factor of *ca.* 80 without major spectral shifts [28]. The introduction of a membrane permeant, esterase-hydrolyzable, pentaacetoxymethylester derivative, fluo-

3:AM, has provided a sound basis for extensive measurements in cytosolic $[Ca^{2+}]_i$ [27, 28].

Measurement of Changes in Cell Volume

The light scattered by a biological object is related to its size, volume, and refractive index relative to that of the surrounding medium. The criterion as to which scattering theory applies mainly depends on the particle size factor $x = 2\pi \cdot r/\lambda$ (ratio between particle radius r and excitation wavelength λ) and on the phase shift factor $p = 2 \cdot x \cdot (m - 1)$, where $m = n_{cell}/n_0$ is the ratio of the refractive indices of the cells (n_{cell}) and their environment (n_0) [29].

In suspension, smooth muscle cells are spherical with a typical diameter of ≈30 μm and a refractive index of 1.37 [20, 30]. Microscopic measurements using ionomycin (10 μM) to equilibrate the extra- and intracellular Ca^{2+} levels indicated that cell contractions caused no deviation from spherical symmetry. Following the recommendation of van de Hulst [29], the scattering pattern of smooth muscle cells can appropriately be characterized by anomalous diffraction theory ($x \gg 1$ and $(m - 1) \ll 1$). Throughout the study, low particle concentrations ($\leq 10^6$/mL) were used to minimize multiple scattering events and to prevent the model from being invalidated.

Neglecting any absorption of light by the cells at the He/Ne laser frequency, the extinction of the cell suspension is related to the decadic scattering extinction coefficient $\epsilon_s(t)$ by Beer's Law:

$$E(t) = -\log_{10}[T(t)] = \epsilon_s(t) \cdot c_0 \cdot d \qquad (1)$$

where $E(t)$ and $T(t)$ correspond to the extinction and transmission data measured as a function of time. c_0 gives the concentration of cells and d the thickness of the sample cuvette.

The relationship between the scattering coefficient $\epsilon_s(t)$ of a spherical particle and cell volume is obtained by integrating the angular scattering intensities over the surface of a sphere [29]:

$$\epsilon_s(t) \propto (n_{cell}(t)/n_{water} - 1)^2 \cdot V(t)^{4/3}/\lambda^2 \qquad (2)$$

where n_{water} and $n_{cell}(t)$ specify the refractive indices of water and of the cells. $V(t)$ gives the cell volume as a function of time and λ corresponds to the wavelength of the He/Ne laser in water ($\lambda = 632.8$ nm/n_{water}).

Measurement of Steady-State Anisotropy

Several fluorescent probes have been proposed for the evaluation of the microviscosity of lipid bilayers. Based on measurements of fluorescence polarization retained after polarized excitation, preference should be given to indicators with collinear absorption and emission dipoles. An excitation with polarized light photoselects those fluorophores whose transition moments happen to be parallel to the electric field of the incident electromagnetic wave. Subsequent to excitation, the depolarization of fluorescence emission is measured and attributed to rotational diffusions of probe molecules during the lifetime of the excited state. The rate and extent of these diffusive motions (i.e., the amount of polarization preserved) depend on the viscosity of the membrane and allow the detection of changes therein. The microviscosity of the membrane is expressed in terms of its steady-state anisotropy $\langle r \rangle$, which is defined by equation (3):

$$\langle r \rangle = \frac{I_{VV} - G \cdot I_{VH}}{I_{VV} + 2 \cdot G \cdot I_{VH}} \qquad (3)$$

After excitation with a vertically polarized laser beam, I_{VV} and I_{VH} give the components of vertically (I_{VV}) and horizontally (I_{VH}) polarized emission intensities. The gain factor, G [$=I_{HV}/I_{HH}$], represents the ratio of the orthogonally polarized fluorescence intensities (I_{HV} and I_{HH}) measured by the detection system at an angle of 90° with respect to a horizontally aligned excitation laser [31].

Steady-state anisotropy, $\langle r \rangle$, defines the degree of fluorescence polarization, and can be related to the microviscosity of the plasma membrane using models such as the Perrin (4) and Stokes-Einstein equations (5) (Ref. 31, p. 135):

$$\text{Perrin equation: } \langle r \rangle = \frac{r_0}{1 + (\tau_F/\phi)} \qquad (4)$$

Here r_0 refers to the anisotropy of the fluorophore measured in a rigid environment, τ_F to its fluorescence lifetime and ϕ to the rotational correlation time of the fluorophore, which depends on the microviscosity (η), temperature (T) and rotational volume of the indicator molecule (V_r):

$$\text{Stokes-Einstein equation: } \phi = \eta \cdot V_r/(R \cdot T) \qquad (5)$$

The measured anisotropy may, thus, be expressed in viscosity units after determination of the rotational volume, V_r, of the fluorophore at a specific temperature and in an isotropic solvent of known viscosity. As related to measurements in cell suspensions, high anisotropy values, $\langle r \rangle$, represent a high viscosity (η) of the plasma membrane, whereas low $\langle r \rangle$ values refer to a high membrane fluidity ($1/\eta$).

Throughout the study, DPH† was used to monitor changes in the microviscosity of the cell membrane. From a physiological point of view, preference should be given to the trimethylammonium derivative of DPH (TMA-DPH)

† *Abbreviations:* AC, adenylate cyclase; DAG, diacylglycerol; DPH, all-*trans* 1,6-diphenyl-1,3,5-hexatriene; G_i, inhibitory G protein; G_s, stimulatory G protein; $InsP_3$, inositol-1,4,5-trisphosphate; MLC, myosin light chain; MLCK, myosin light chain kinase; PI, phosphatidylinositol; PIP, phosphatidylinositol-4-monophosphate; PIP_2, phosphatidylinositol-4,5-bisphosphate; PLC, phospholipase C; PKA, protein kinase A; PKC, protein kinase C; TMA-DPH, 1-[4-(trimethyl-ammonium)phenyl]-6-phenyl-1,3,5-hexatriene.

to reflect uniquely plasma membrane properties, because it is known that this indicator remains localized in the plasmalemma [32]. However, because TMA-TPA is virtually nonfluorescent in water and the amount of probe bound to the lipid bilayer varies in proportion to the available membrane surface, the fluorescence signal follows biochemical events resulting from membrane swelling, fusion, or contraction. The manufacturer of TMA-DPH (Molecular Probes), therefore, recommends not using this indicator for microviscosity measurements if contractions occur simultaneously. DPH rapidly partitions into the acyl side-chain region of lipid bilayers and has a broad absorption band with a maximum near 355 nm and a high extinction coefficient of *ca.* 80,000 $M^{-1} \cdot cm^{-1}$. Between 320 and 380 nm, the limiting anisotropy, r_0, does not depend on the excitation wavelength, and the excitation and emission dipole moments happen to be almost parallel to each other (α = 6.6°) (i.e., r_0 = 0.392) [33].

For randomly distributed sample molecules, anisotropy, $\langle r \rangle$, may, thus, vary between 0.0 and 0.392. Due to the random orientation of the sample molecules and the photoselection of excitation, the r_0 value is considerably smaller than that possible for scattered light, r_0 = 1.0 [31]. In most lipid bilayers, DPH behaves like an unhindered isotropic rotator at a temperature of 37°C. However, various studies indicate that the rotational motion of DPH may be hindered if the phase transition temperature of the membrane is significantly higher than 25°C [33]. Because this would invalidate the Perrin and Stokes-Einstein equations, the measured $\langle r \rangle$ values throughout the paper are expressed in anisotropy units, not transformed into standard viscosity units (cP).

EXPERIMENTAL

Incubation with the Ca^{2+} Indicator Fluo-3, DPH, and Formoterol

Approximately 10^7 cells/mL were incubated with 10 μM fluo-3:AM and 5 μM DPH in the presence of 1.3 mM Ca^{2+} (40 min; 37°C). After the incubation period, the cells were centrifuged (70 *g*; 5 min; 25°C) and resuspended at a concentration of 10^6 cells/mL in a buffer solution that contained the following ingredients in physiological concentrations: 1.3 mM $CaCl_2$, 135 mM NaCl, 5 mM KCl, 1 mM Na_2HPO_4, 1 mM $MgCl_2$ and 5 mM D-glucose, buffered to a pH of 7.4 with 10 mM HEPES/HCl [34, 35]. Thereafter, the cell suspension was subdivided into 2 parts. To give the intracellular esterases sufficient time to cleave the incorporated pentaacetoxymethylester derivatives of fluo-3, both cell fractions were postincubated (40 min; 37°C) in the absence (control cell group) or presence of 50 nM formoterol. Finally, the cells were centrifuged and resuspended at a density of 10^6 cells/mL in the saline buffer solution containing the appropriate formoterol concentration (0 or 50 nM) to prevent a partitioning of formoterol into the buffer medium and, thereby, maintain steady-state conditions during the experiment.

Noticeably, radioligand studies clearly indicated that the densities of surface receptors for angiotensin II and the β_2-adrenoceptor agonist formoterol were identical in both cell batches [36].

Apparatus for the Simultaneous Measurements of Changes in the Cytosolic Ca^{2+} Concentration, Cell Volume, and Microviscosity of the Plasma Membrane

The experimental layout of the apparatus is schematically displayed in Fig. 1. As shown, 3 different laser systems were used simultaneously. The output of each laser was focused on a distinct optical fiber that was highly transparent for its specific wavelength. Finally, the 3 fiber optic bundles were coherently [37] bound together using epoxy, and conducted the laser light to the sample chamber that contained a thermostatted (37°C) and magnetically stirred 1-cm sample cuvette. Remarkably, the optical fiber totally destroyed the polarization of the laser beams so that its output was com-

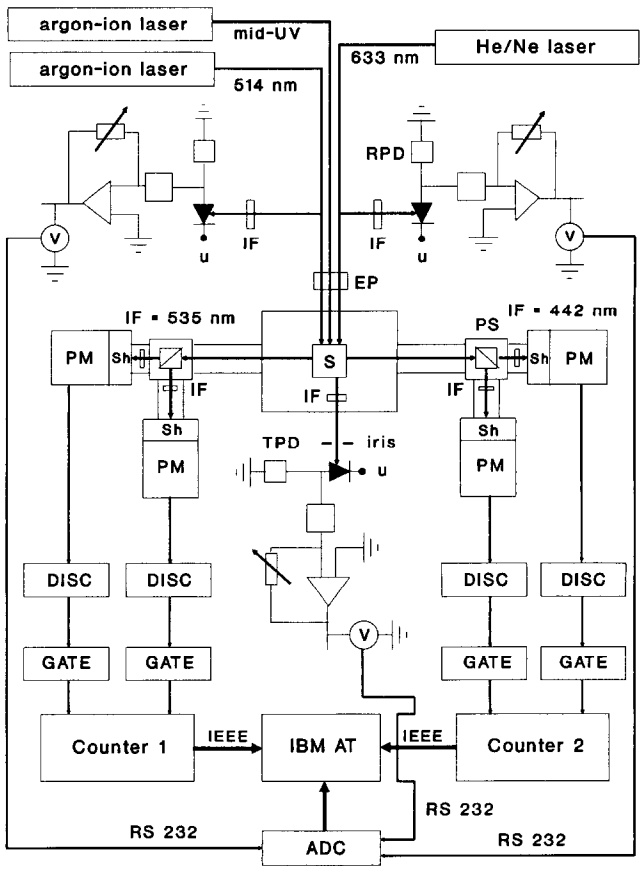

FIG. 1. Schematic experimental setup for the simultaneous measurement of angiotensin II-induced Ca^{2+} transients and changes in the cell volume and microviscosity of the plasma membrane. The diverse optical elements employed to focus the laser beams and to collect the fluorescence photons are not shown in the Fig. The abbreviations have the following meanings: ADC, analog-to-digital converter; EP, excitation polarizer; IF, interference filter; PM, photomultiplier; PS, polarizing beam splitter cube; RPD, reference photodiode; Sh, shutter; TPD, transmission photodiode.

pletely unpolarized. Consequently, an electronically positioned (Kuhnke; Dietlikon, Switzerland; D59-BOR-F-DS-9420) excitation polarizer (Wild & Leitz; Zurich, Switzerland; 033712) was used to polarize the lasers at the entrance of the sample chamber to enable the anisotropy measurements to be carried out. The fiber optical system and the optics (various lenses) employed to focus the diverse lasers into the sample chamber are not shown in Fig. 1.

Prior to starting the experiment, the excitation polarizer and the polarizing beam splitter cube were precisely positioned in the vertical and horizontal orientations to allow accurate measurements of the fluorescence anisotropy. In addition, the determination of the gain factor, G, was required to calculate the steady-state anisotropy from the spectroscopic data obtained, (as in Eqn (3)).

Alignment of the Excitation/Emission Polarizers

The positions of the excitation polarizer and the polarizing beam splitter cube were carefully aligned using a solution of glycogen in water ($\langle r \rangle$ = 1.0) and 9-cyanoanthracene in pure ethanol ($\langle r \rangle$ = 0.0). Details concerning the alignment procedure are found in Ref. 31, p. 131.

Determination of the Gain Factor G

After excitation with a horizontally polarized and power-locked argon-ion laser (Spectra Physics, SP 2045-15S, mid UV range: 351.1–363.8 nm, beam diameter = 6 mm), the vertically (I_{HV}) and horizontally (I_{HH}) polarized fluorescence intensities (Corion, IF-filter, λ = 442 nm, FWHM = 10 nm) from the DPH-pretreated cell suspensions were registered (method: see below) within a time interval of 5 sec and the autofluorescence-corrected G factors calculated from the equation $G = I_{HV}/I_{HH}$.

The Measurement Cycle

Subsequent to the alignment of the excitation/emission polarizers and the determination of the gain factor, G, the experiment was begun. Notably, the Ca^{2+} transient and changes in the cell volume and microviscosity of the plasma membrane were measured simultaneously.

Measurement of the Ca^{2+} Transient

The 514.5-nm line of an argon-ion laser (Spectra Physics, SP 165-09) was selected to excite fluo-3 near its excitation maximum and to record angiotensin II (20 nM)-induced changes in cytosolic Ca^{2+} concentration. The light photons emitted from the Ca^{2+} indicator fluo-3 (Corion, IF-filter, λ = 535 nm, FWHM = 10 nm) were collected at an angle of 90°, detected by two photomultiplier tubes operating in the single-photon-counting mode (Hamamatsu, R 928) and monitored by a two-channel single-photon-counting unit (Stanford Research System, SR 400). A disadvantage of the photon-counting method is its limited range of intensity over which count rates are linear. Nevertheless, the signal-to-noise ratio increases with the square root of the number of photons observed. To retain the advantages of the single-photon-counting vs the analog detection mode, without reducing emission intensity (using neutral density filters), the fluorescence emitted from free and Ca^{2+}-complexed fluo-3 was divided by a beam splitter cube (Laser components, PCBD10) and registered by two separate photomultipliers. To further improve the signal-to-noise ratio, the photon counter was equipped with adjustable discriminators that distinguished between real pulses and background noise. Typically, the incoming pulses were accumulated within a time interval (=gate) of 0.5 sec. At the end of each measurement cycle, the count rates (photons/sec) were transferred *via* an IEEE interface to an IBM-AT computer and averaged over the two detection channels used.

As shown in Fig. 1, fluctuations in the power of the argon-ion laser were continuously monitored by a dedicated photodiode (EG & G, UV-250-BQ) used to subsequently normalize the fluorescence signals obtained. The photodiode signal was processed by a low-noise current-to-voltage converter (UDC, 101C), digitized by a variable gain analog-to-digital I/O interface (Metrabyte, DAS-8 PGA) and stored on the IBM-AT computer, which also controlled the single photon counter.

At the end of each individual scan, the fluorescence signals were calibrated by addition of ionomycin (10 μM), Ca^{2+} (1 mM) and Mn^{2+} (4 mM) [25, 28, 38]. Typically, the cells remained active vs an angiotensin II (20 nM) stimulus for a maximum of 6 hr.

Measurement of Changes in Cell Volume

Simultaneously with the registration of the Ca^{2+} transient, the angiotensin II (20 nM)-induced cell volume time-course was recorded. Light transmission measurements were performed at 632.8 nm, where the cells scatter but do not absorb light, using a vertically polarized, frequency-stabilized He/Ne laser (Spectra Physics, SP 106-1). The laser beam was expanded to a Gaussian (1/e) diameter of 6 mm to increase the number of cells under observation and crossed, unfocused, the sample cuvette. All transmission measurements were carried out in the ratio mode (transmission: $T = I(t)/I_0(t)$, where $I_0(t)$ gives the incident and $I(t)$ the transmitted intensity as a function of time). To isolate the He/Ne wavelength, two interference filters (Corion, IF-filters, λ = 632.8 nm, FWHM = 1 nm) were used in front of reference and transmitted light detectors (EG & G, UV-444B photodiodes). A small (3 mm diameter) iris placed in front of the transmission detector was used to prevent forward-scattered light from the cells from reaching the detector. Because both the reference and the transmission photodiodes only measured a fraction of the light intensities $I_0(t)$ and $I(t)$, the signals were amplified to obtain reasonable values (error $\leq$ 0.2%) for the transmission data.

The addition of the Ca^{2+} ionophore ionomycin (10 μM)

equilibrated the extra- and intracellular Ca^{2+} levels [20] and caused a sustained contraction of the cells. To test the mathematical model used, aliquots of the cell suspension were analyzed on a high-precision microscope (Reichert-Jung Polyvar MET) by measuring the diameter of 100 cells before and after addition of ionomycin at various Ca^{2+} concentrations, ranging from 100 nM to 1.3 mM.

Measurement of Changes in Microviscosity

A vertically polarized and power-locked argon-ion laser beam (Spectra Physics, SP 2045-15S, mid UV range: 351.1–363.8 nm, diameter = 6 mm) was used to excite the DPH molecules located in the cell membranes. Thereafter, the vertically (I_{VV}) and horizontally (I_{VH}) polarized emission intensities were measured using an interference filter (Corion, IF-filter, λ = 442 nm, FWHM = 10 nm) to select the wavelength and a polarizing beam splitter cube (Newport, 10FC16.PB3) to separate the orthogonally polarized fluorescence components. Detected by 2 separate photomultipliers operating in the single-photon-counting mode (Hamamatsu, R 928), the photoelectrons released from the individual detection tubes were registered by a two-channel single-photon-counting unit (Stanford Research System, SR 400). At the end of each measurement cycle, the count rates (photons/sec) were transferred to the IBM-AT computer that controlled the entire experiment.

To obtain reasonable values for the anisotropy parameter, $\langle r \rangle$, the autofluorescences (I_{HV}, I_{HH}, I_{VV} and I_{VH}) of unlabeled cells (stemming mainly from $NADP^+$ and NADPH) and of cells pretreated with 50 nM formoterol were determined in a preliminary experiment and subtracted from the data set obtained. Because DPH and formoterol partition into similar regions of the plasma membrane, it was also necessary to show that the β_2-adrenoceptor agonist did not quench the fluorescence emission of DPH. In addition, changes in autofluorescence, which could be triggered by the injection of angiotensin II into the cell suspension through the generation of fluorescent or fluorescence-quenching reaction products, had to be monitored.

RESULTS

Changes in Angiotensin II-Induced Ca^{2+} Transients

A modified Bateman function was used to fit the experimental data and obtain physiologically meaningful constants that characterize the angiotensin II-induced Ca^{2+} transient, as in Eqn (6). The model takes exponential behavior into account as follows:

$$[Ca^{2+}]_i \text{ (nM)} = C_1 \cdot [2^{-(t-t_0)/\tau_{el}} - 2^{-(t-t_0)/\tau_{in1}}] + C_2 \cdot [1 - 2^{-(t-t_0)/\tau_{in2}}] + C_3;\ t \geq t_0 \qquad (6)$$

The parameters C_1 and C_2 (nM) correspond to the maximal increase in cytosolic Ca^{2+} concentration induced by an intracellular release of Ca^{2+} and by an enhanced influx through the plasma membrane, respectively. The onset of Ca^{2+} release is specified by t_0 (sec). τ_{el} (sec) characterizes the Ca^{2+}-half-life elimination constant associated with the transient phase of the Ca^{2+} signal and τ_{in1}, τ_{in2} (sec) the half-life rise times of the individual Ca^{2+} pathways. Finally, C_3 (nM) corresponds to the basal Ca^{2+} concentration prior to stimulation with angiotensin II.

The fitting function is based on the idea that two different processes dominate the release and reuptake of Ca^{2+}. The first mechanism (first bracket) characterizes the $InsP_3$-induced intracellular liberation and sequestration of Ca^{2+}. The second bracket corresponds to the rise in cytosolic Ca^{2+} concentration caused by a stimulus-induced increase in the permeability of Ca^{2+} channels located in the plasma membrane.

The basal cytosolic Ca^{2+} concentration (C_3) of control cells, 160 nM (±4 nM), was in excellent agreement with earlier data measured in suspension [22], but significantly lower for those cells pretreated with formoterol (50 nM). To obtain reliable Ca^{2+} measurements, antifluorescein IgG antibodies were used to quench extracellular fluorescence, because a leakage of fluo-3 through the cell membrane and/or disintegration of the cells increases fluorescence intensity and falsifies the results (Table 1).

As shown in Figs. 2 and 3 (upper panel), the angiotensin II-induced Ca^{2+} response was much higher in control cells and clearly suppressed in the presence of 50 nM formoterol. Formoterol-pretreated cells showed a reduced response, both of the first and second Ca^{2+} pathways. Cytosolic Ca^{2+} concentration in smooth muscle cells remained elevated over a long time period after stimulation with angiotensin II. Contrasting these results, the net influx of Ca^{2+} from the extracellular space was lowered in a dose-dependent manner in formoterol-pretreated cells (data not shown) and became negligible at a formoterol concentration of 50 nM. As shown in Table 1, the time constants τ_{in1} (sec) tended to be somewhat smaller for formoterol-pretreated cells and

TABLE 1. Effect of formoterol (50 nM) on angiotensin II (20 nM)-induced Ca^{2+} transients of vascular smooth muscle cells

Constant	Cells	Samples	Mean	SD
Max. response* (mainly C_1)	formoterol	19	59.5 nM	2.9 nM
	control	20	134.0 nM	4.0 nM
C_2	formoterol	19	0.4 nM	0.1 nM
	control	20	14.5 nM	0.8 nM
τ_{el}	formoterol	19	9.6 sec	0.7 sec
	control	20	14.5 sec	0.8 sec
C_3	formoterol	19	136.1 nM	4.1 nM
	control	20	160.2 nM	3.9 nM
τ_{in1}	formoterol	19	3.0 sec	0.3 sec
	control	20	4.1 sec	0.3 sec
τ_{in2}	formoterol	19	27.2 sec	3.2 sec
	control	20	8.2 sec	1.8 sec

The function used to fit the experimental data is given in the text, Eqn (6).

* C_1 corresponds to the maximal increase in cytosolic Ca^{2+} induced by a release of $InsP_3$ in the absence of any elimination processes. If $\tau_{in1} \ll \tau_{el}$ and $\tau_{in1} \ll \tau_{in2}$, C_1 is equal to the maximal response.

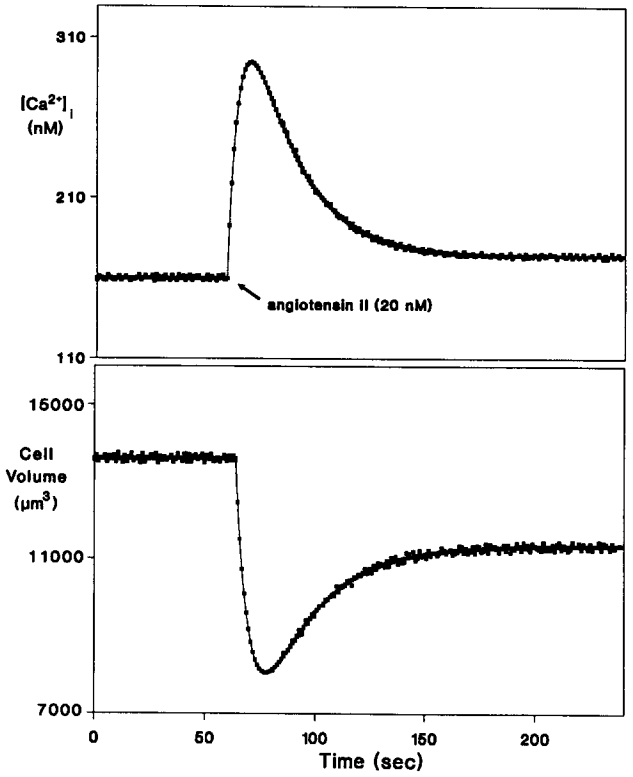

FIG. 2. Ca^{2+} response and volume contraction of control cells. The angiotensin II (20 nM)-induced Ca^{2+} response (upper trace) is presented simultaneously with the variation in its cell volume (lower trace). The *x*-axis corresponds to the time-scale in both figures. The *y*-axis of the upper panel gives the cytosolic Ca^{2+} concentration, the *y*-axis of the lower panel the apparent cell volume. Dotted points correspond to the experimentally observed data, the line to the theoretically predicted transients using the model functions, Eqn (6) and (9), given in the text. One can clearly recognize that, in the control cell group, there is a timelag of approximately 4.7 sec between the onset of Ca^{2+} release and the initiation of cell contraction.

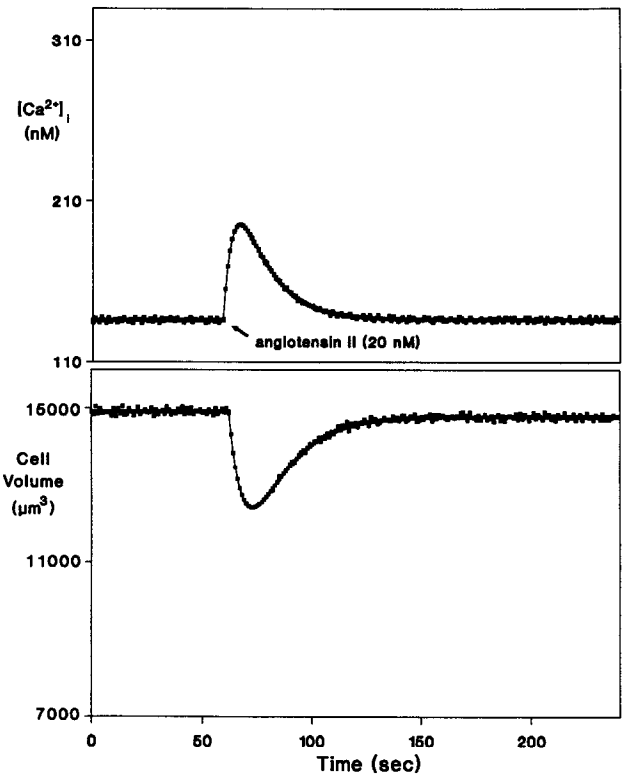

FIG. 3. Ca^{2+} response and volume contraction of formoterol (50 nM)-pretreated cells. In analogy to Fig. 2, the angiotensin II (20 nM)-induced Ca^{2+} response (upper trace) of the cells is presented simultaneously with the variation in its cell volume (lower trace).

the rate of Ca^{2+} influx ($1/\tau_{in2}$) through the plasma membrane was clearly faster in the control cell group. In the presence of 50 nM formoterol, the elimination of Ca^{2+} ($1/\tau_{el}$) from the cytoplasm was enhanced and cytosolic Ca^{2+} concentration decreased almost to the starting value. In both cell groups, the covariance matrix implied strong correlations between the various fitting constants in Eqn (6) and, especially, between the two Ca^{2+} pathways involved.

Changes in Angiotensin II-Induced Cell Volume Transients

As outlined above, cell volume was obtained by measuring light transmission at a wavelength not absorbed by cellular components, and by relating the calculated extinction to the theoretical scattering coefficient [$\epsilon_s(t)$].

Based on the assumption that the refractive index of smooth muscle cells [$n_{cell}(t)$] does not change considerably during the process of contraction [as in Eqn (1) and (2)], the scattering coefficient $\epsilon_s(t)$ depends on the 4/3 power of the cell volume and extinction data may be used to calculate the cell volume time-course from Eqn (7):

$$E(t) = k_1(n_{cell}, c_0, \lambda) \cdot V(t)^{4/3} \quad (7)$$

The constant $k_1(n_{cell}, c_0, \lambda)$ in Eqn (7) was determined by taking into account the initial extinction [$E(t = 0)$] and the microscopically measured cell volume (V_0) prior to stimulation with angiotensin II (Eqn (8) and Table 2):

$$k_1(n_{cell}, c_0, \lambda) = E(t = 0)/V_0^{4/3} \quad (8)$$

Subsequently, all extinction data [$E(t)$] were numerically fitted to Eqn (7) and the apparent cell volume, together with its derivative (i.e., speed of contraction), calculated as a function of time (Figs. 2 and 3, lower panels).

As mentioned above, ionomycin was added at the end of each experiment to equilibrate the extra- and intracellular Ca^{2+} concentrations and to induce a sustained contraction of the cells [20]. Because the theoretically predicted and microscopically measured cell volumes of both native and ionomycin-pretreated cells were identical within an experimental error of approximately 3%, we concluded that the chosen mathematical approach gives reasonable estimates of actual cell volume.

TABLE 2. Effect of formoterol (50 nM) on angiotensin II (20 nM)-induced changes in the cell volume of smooth muscle cells*

Constant	Cells	Samples	Mean	SD
V_0	formoterol	100	14910 μm^3	110 μm^3
	control	100	13630 μm^3	105 μm^3
r_0	formoterol	100	15.27 μm	0.04 μm
	control	100	14.82 μm	0.04 μm
V_{min}	formoterol	19	12430 μm^3	95 μm^3
	control	20	8070 μm^3	100 μm^3
r_{min}	formoterol	19	14.37 μm	0.04 μm
	control	20	12.44 μm	0.05 μm
$[dV/dt]_{max}$	formoterol	19	−1240 μm^3/sec	75 μm^3/sec
	control	20	−1660 μm^3/sec	85 μm^3/sec
$[dr/dt]_{max}$	formoterol	19	−0.44 μm/sec	0.03 μm/sec
	control	20	−0.63 μm/sec	0.03 μm/sec
V_{final}	formoterol	19	14780 μm^3	105 μm^3
	control	20	11340 μm^3	95 μm^3
r_{final}	formoterol	19	15.22 μm	0.04 μm
	control	20	13.94 μm	0.04 μm

The function used to fit the cell volume transients is given in the text, Eqn (9).

* The standard deviations (SD) give the precision of the measurements relative to the microscopically determined cell volumes of control and formoterol (50 nM)-pretreated cells; the absolute accuracy (but not the differences in cell volume) may be lower by a factor of approximately three. The symbols V_0 and r_0 refer to the initial cell volume and radius of the cells determined by microscopic measurements [20]. V_1 corresponds to the maximal decrease in cell volume induced by a release of Ca^{2+} from intracellular stores in the absence of any relaxation processes. If $\tau_{c1} \ll \tau_{rel}$ and $\tau_{c1} \ll \tau_{c2}$, V_1 is equal to $-[V_0 - V_{min}]$ and V_2 matches $-[V_0 - V_{final}]$.

Following the idea of Murray [39], two different processes control the contraction of smooth muscle cells. Consequently, the cell volume transients were fitted to Eqn (9):

$$V(t) = V_1 \cdot [2^{-(t-t_1)/\tau_{rel}} - 2^{-(t-t_1)/\tau_{c1}}] + V_2 \cdot [1 - 2^{-(t-t_1)/\tau_{c2}}] + V_3;\ t \geq t_1 \quad (9)$$

The parameters V_1 and V_2 (μm^3) correspond to the maximal decrease in cell volume caused by a transient and sustained contraction of the cells, respectively. t_1 (sec) gives the time point at which the cells start to contract. τ_{rel} (sec) specifies the time-constant leading to a relaxation of the contracted cells and τ_{c1}, τ_{c2} (sec) characterize the time progression of the transient and sustained phases of contraction. Finally, V_3 (μm^3) designates initial cell volume prior to stimulation with angiotensin II.

As outlined below, the first mechanism (first bracket) characterizes the contraction induced by a release of Ca^{2+} from intracellular sources, whereas the second term describes the tonic phase of contraction associated with a Ca^{2+} influx through receptor-operated (ROCC) Ca^{2+} channels located in the plasma membrane. The subdivision of the contraction process into two distinct mathematical functions does not mean that the mechanisms act independently of each other. On the contrary, the covariance matrix implies strong correlations between the two phases of contraction.

The variation in cell volumes of formoterol (50 nM)-pretreated and control cells are displayed in Figs. 2 and 3 (lower panels). The associated fitting parameters characterizing these transients are summarized in Tables 2 and 3. Significant differences were observed between the two cell fractions. In agreement with the observation that basal cytosolic Ca^{2+} concentration was lower in formoterol-pretreated cells prior to stimulation with angiotensin II, their initial cell volume was slightly larger than that of control cells. In addition, formoterol-pretreated cells contracted slower ($[dV/dt]_{max}$; −25 ± 5%) and to a minor extent ($[V_0 - V_{min}]$; −55 ± 3%). As displayed in Figs. 2 and 3, control cells remained in a contracted state and relaxed only partially within the time-frame of the experiment ($(V_0 - V_{final})/[V_0 - V_{min}]$ = 41 ± 3%). In contrast, formoterol-pretreated cells almost completely relaxed to their initial cell volume. The time constants τ_{rel}, which characterize the relaxation of the transient phase of contraction, were in both cell fractions somewhat larger (+≈10%) than the decay times τ_{el} assigned to the transient Ca^{2+} signal. The parameters τ_{c2}, defining the time progression of the sus-

TABLE 3. Effect of formoterol (50 nM) on the various time constants, in Eqn (9), and on the time delay between Ca^{2+} release and cell contraction

Constant	Cells	Samples	Mean	SD
τ_{rel}	formoterol	19	10.9 sec	0.9 sec
	control	20	16.2 sec	1.0 sec
τ_{c1}	formoterol	19	5.2 sec	0.4 sec
	control	20	4.2 sec	0.4 sec
τ_{c2}	formoterol	19	24.6 sec	3.0 sec
	control	20	8.5 sec	2.4 sec
Time delay ($t_1 - t_0$)	formoterol	19	3.0 sec	0.4 sec
	control	20	4.7 sec	0.3 sec

tained phase, closely matched the time constants τ_{in2} representing the Ca^{2+} influx from the extracellular space. As shown in Table 3, pretreatment with formoterol had a considerable effect on the time delay between the onset of Ca^{2+} release and the induction of the contractile response. Formoterol, obviously, contributes to a faster transduction of the angiotensin II-mediated signal to the contractile elements of the cell. Contrasting these results, the speed of contraction (characterized by the variables $[dV/dt]_{max}$ and $1/\tau_{c1}$) tended to be somewhat slower after pretreatment with 50 nM formoterol.

Results from the Anisotropy Measurements

Measurements using paraffin oil as reference solvent demonstrated that formoterol, in concentrations up to 50 μM, did not quench the fluorescence emission of DPH. In addition, no change in the autofluorescences of the cell suspensions was observed after stimulation with angiotensin II concentrations up to 100 nM.

As mentioned above, the autofluorescences (I_{HV}, I_{HH}, I_{VV} and I_{VH}) of unlabeled and of formoterol (50 nM)-pretreated cells were determined in a preliminary experiment and subtracted from the data set obtained to procure reasonable estimates for the anisotropy values, $\langle r \rangle$. Finally, steady-state anisotropy, $\langle r \rangle$, was calculated as a function of time for those cells pretreated with formoterol (50 nM) and for those representing the control cell group.

An injection of angiotensin II (20 nM) into the cell suspension caused no detectable changes in the microviscosity of the plasma membrane in either cell fraction. Obviously, the quantity of lipids transformed by the breakdown of phosphoinositides was too small to significantly alter the microviscosity of the cell membrane. This result is in reasonable harmony with the fact that the overall phosphoinositide content of the plasma membrane only varies between 2% and 8% [40, 41]. In addition, angiotensin II-induced activation of phospholipase C specifically catalyzes the breakdown of phosphatidylinositol-4,5-bisphosphate (PIP_2) and, to a minor extent, of phosphatidylinositol-4-monophosphate (PIP) and of phosphatidylinositol (PI) [41].

Even though no transient variations in membrane microviscosities could be detected after stimulation with angiotensin II, the steady-state anisotropy (−18 ± 1%) and, therefore, the microviscosity of the plasma membrane were significantly lower after pretreatment with 50 nM formoterol (Table 4).

Recently, the membrane/water partition constant of formoterol has been measured using dioleoyl-phosphatidylserine and 1-palmitoyl-2-oleoyl-phosphatidylcholine (1:9) as artificial membrane lipid components reconstituted as uni- and/or multilamellar liposomes ($\log_{10}(K_{pmem})$ = 2.74 ± 0.04; pH = 7.0; 20°C) [42]. As expected from the microviscosity measurements, formoterol strongly accumulates in lipid bilayers.

TABLE 4. Effect of formoterol (50 nM) on the steady-state anisotropy, $\langle r \rangle$, of smooth muscle cells

Constant	Cells	Samples	Mean	SD
$\langle r \rangle$	formoterol	19	0.210	0.003
$\langle r \rangle$	control	20	0.255	0.002

The injection of angiotensin II (20 nM) into the cell suspension caused no detectable changes in membrane microviscosity in either cell fraction. The quantity of lipids transformed by the breakdown of the phosphoinositides was obviously too small to significantly alter the fluidity of the plasma membrane.

DISCUSSION

Several inflammatory mediators, such as histamine, prostaglandins, hydroxyeicosatetraenoic acid, and the sulfidopeptide leukotrienes (LTC_4, LTD_4, and LTE_4), have been implicated in the pathogenesis of asthma. Most of these endogenous mediators, which play a dominant role in the initiation of the asthmatic reactions, are potent bronchoconstrictors mainly through an enhanced breakdown of phosphatidylinositol-4,5-bisphosphate (PIP_2) and the subsequent intracellular release of inositol-1,4,5-trisphosphate ($InsP_3$) and diacylglycerol (DAG). $InsP_3$ mobilizes Ca^{2+} from internal stores and DAG activates protein kinase C (PKC) [43]. The interplay of these intracellular messengers mediates a wide variety of cellular responses. Angiotensin II causes an immediate activation of phospholipase C (PLC) *via* a specific, stimulatory guanine nucleotide binding protein (G_q) [41, 44] and instantaneously triggers the hydrolysis of phosphatidylinositol-4,5-bisphosphate (PIP_2). Applied as model substance for the stimulation of the phosphoinositide-PLC pathway, angiotensin II has been utilized to simulate the bronchospasm in smooth muscle cells [20]. Apart from its action on the phosphoinositide-PLC pathway, angiotensin II is known to mildly activate the inhibitory G protein (G_i) that is coupled to adenylate cyclase and downregulates its activity [41, 45].

It is well accepted today that β_2-adrenoceptor agonists reverse airway obstructions in asthmatics, primarily by relaxing airway smooth muscle [46]. Agonist-bound β_2-adrenoceptors strongly activate adenylate cyclase through a stimulatory guanyl nucleotide binding protein (G_s) and overcome the inhibitory effect of angiotensin II on adenylate cyclase in a dose-dependent manner [6, 47].

In the resting state, the G_s protein consists of three subunits, $\alpha_s \cdot GDP$ (45 kDa), β (35 kDa), and γ (7 kDa), which form the stable protein complex $\alpha_s \cdot GDP \cdot \beta\gamma$ [48, 49]. The attachment of formoterol to the β_2-receptor (64 kDa) leads to a conformational change in the three-dimensional structure of the β_2-adrenoceptor glycoprotein, which subsequently activates the G_s protein. This interaction promotes the release of GDP from the α_s subunit with a successive binding of GTP and dissociation of the $\alpha_s \cdot GTP \cdot \beta\gamma$ complex into a stimulatory $\alpha_s \cdot GTP$ component and a $\beta\gamma$ heterodimer. $\alpha_s \cdot GTP$ migrates along the lipid bilayer to the active site of adenylate cyclase and catalyzes the formation of cAMP. Notably, the $\alpha_s \cdot GTP$

subunit has an intrinsic GTPase activity ($\tau \approx 10$ sec), which hydrolyzes bound GTP to GDP and impairs the catalytic activity of $\alpha_s \cdot$ GTP. The cycle is completed by reassociation of the $\alpha_s \cdot$ GTP with the $\beta\gamma$ component. The increased fluidity of the plasma membrane in formoterol (50 nM)-pretreated cells supposedly accelerates the lateral motion of the stimulatory $\alpha_s \cdot$ GTP unit to the binding site(s) of adenylate cyclase before the $\alpha_s \cdot$ GTP complex becomes inactivated by its intrinsic GTPase activity. In addition, the internal motions of the groups and peptide chains of adenylate cyclase, which are connected to its biochemical function, are clearly enhanced in an environment of higher fluidity [40, 50].

The stimulation of β_2-adrenergic receptors, thus, increases the generation of cAMP and subsequently activates the cAMP-dependent protein kinase A (PKA) that phosphorylates myosin light-chain kinase (MLCK) [47]. Compared to native MLCK, the phosphorylated product exhibits a lower affinity for the calmodulin-Ca_4^{2+} complex, causing a decrease in the phosphorylation of 20 kDa myosin light chains and a reduction in actin-myosin coupling [51]. Phosphorylation of the myosin light chain results in an activation of actin-dependent Mg^{2+} ATPase, which ultimately leads to tension development [52]. A rise in cAMP also acts to decrease Ca^{2+} influx through the plasma membrane [6, 53], to catalyze the sequestration of Ca^{2+} into intracellular storage sites, and to stimulate extrusion *via* Ca^{2+} ATPase into the extracellular space [54]. In addition, cAMP has been shown to inhibit phospholipase C-mediated phosphoinositide hydrolysis so that the angiotensin II-induced formation of $InsP_3$ and DAG is suppressed and the mobilization of Ca^{2+} from internal stores, consequently, lowered [55]. Analogous to its function in mesangial cells, Ca^{2+} is assumed to occupy a central role in excitation-contraction coupling in smooth muscle cells by initiating the Ca^{2+}-calmodulin-dependent processes [6, 20] (Fig. 4).

The administration of analogs of cAMP and the effect of forskolin, a direct stimulator of adenylate cyclase, demonstrate that an increase in intracellular cAMP amplifies the

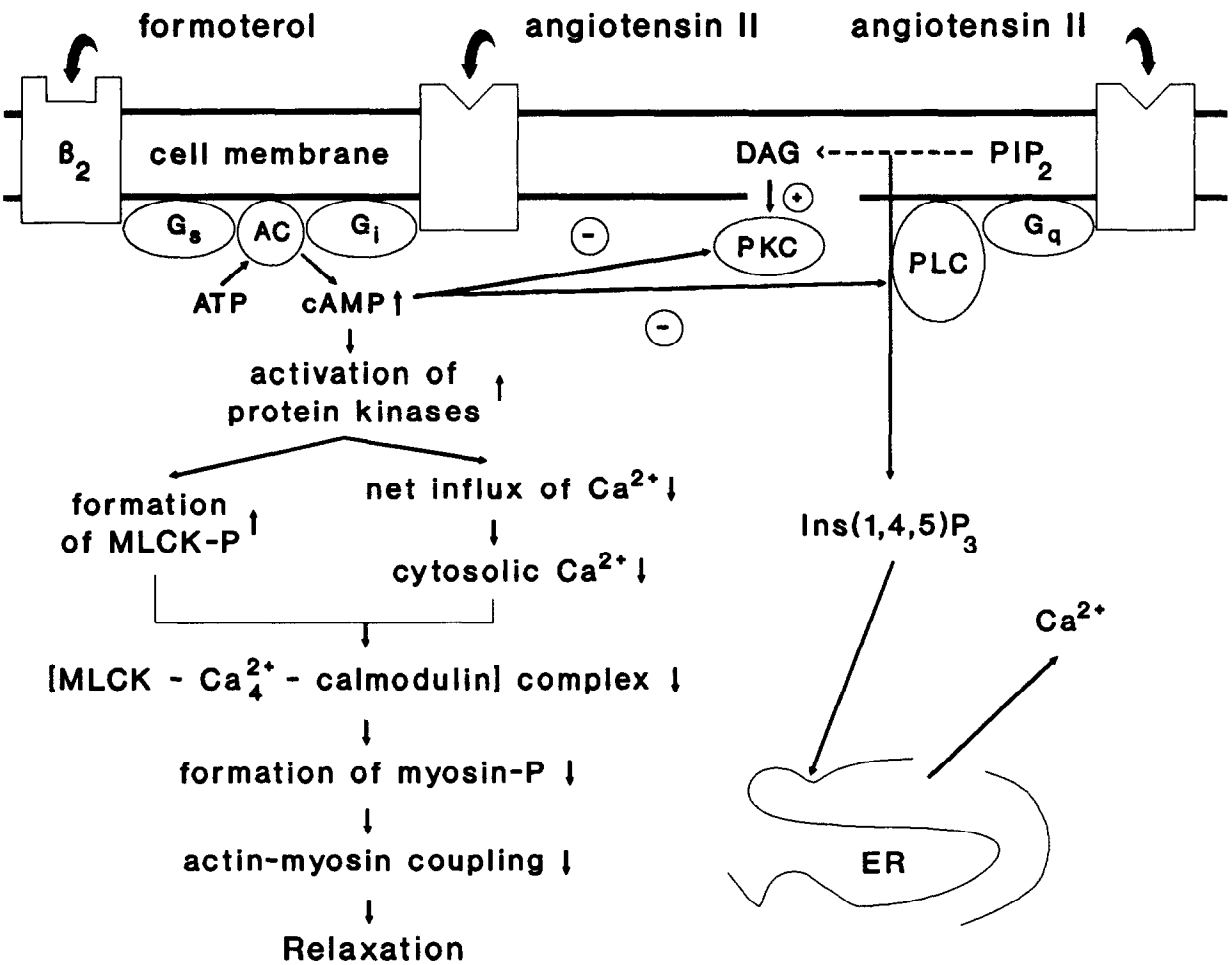

FIG. 4. Cellular processes responsible for the β_2-adrenoceptor-mediated relaxation of smooth muscle cells after a challenge with angiotensin II (20 nM). A detailed discussion of the biochemical processes and all abbreviations are given in the text. For reasons of simplicity, the stimulating effect of cAMP on nitric oxide synthesis and the subsequent generation of relaxant cGMP is not shown in the Fig.

transcription and expression of the inducible nitric oxide synthase gene in smooth muscle cells and, consequently, the synthesis of nitric oxide through the L-arginine/L-citrulline pathway [56]. Nitric oxide is a potent activator of the soluble guanylate cyclase and substantially elevates the intracellular level of cGMP. cAMP and cGMP contribute synergistically to the relaxation of smooth muscle by phosphorylation of MLCK and stimulation of the Ca^{2+} ATPase responsible for the extrusion of Ca^{2+} [57]. Even though the inducible nitric oxide synthase of smooth muscle cells possesses calmodulin recognition sites, the enzyme is, surprisingly, neither stimulated by Ca^{2+} nor blocked by calmodulin antagonists [58].

It is well known that β_2-stimulating agents lead to a hyperpolarization of the resting membrane potential in smooth muscle cells mainly through an activation of ATP-sensitive K^+ channels [59] and a stimulation of high-conductance, Ca^{2+}-activated K^+ channels [60]. Both effects are mediated either by phosphorylations of channel proteins *via* cAMP-dependent PKA or by activation of ion channels through the $\alpha_s \cdot$ GTP subunit of the stimulatory G protein (G_s). Notably, the increased fluidity of the plasma membrane in formoterol-pretreated cells supposedly enhances the coupling between the $\alpha_s \cdot$ GTP component and the associated ion channels. Moreover, the β_2-adrenergic increase in the permeability of K^+ channels is tightly coupled with a PKA-activated stimulation of Na^+/K^+-ATPase [61, 62]. Measurements using the membrane sensitive dye 3,3'-diethylthiacarbocyanine iodide indicated that the resting membrane potential of the smooth muscle cells was -53.2 ± 1.2 mV ($n = 15$) in the control cell group. A formoterol (50 nM)-induced hyperpolarization was apparent in all cell batches and averaged 12.1 ± 1.5 mV ($n = 12$) [63]. Details on the measurement technique used have been published previously [64].

Our experimental data are in excellent agreement with the given theoretical background information. The cAMP-related inhibition of Ca^{2+} influx and the faster intracellular sequestration and catalyzed extrusion of Ca^{2+} *via* the Ca^{2+} ATPase consistently explain the lower basal Ca^{2+} level in formoterol (50 nM)-pretreated cells. Moreover, the formoterol-associated hyperpolarization reduced Ca^{2+} influx through voltage-operated Ca^{2+} channels [65] and the Na^+/Ca^{2+} exchanger probably enhanced the extrusion of Ca^{2+} into the extracellular space to compensate for the higher Na^+ gradient caused by an increased activity of Na^+/K^+-ATPase [61, 62]. Resulting from the decrease in cytosolic Ca^{2+} and the reduced phosphorylation of the myosin light chain, the initial cell volume of formoterol-pretreated cells (prior to stimulation with angiotensin II) was slightly larger than that of control cells. As expected from theoretical considerations, the angiotensin II-induced Ca^{2+} response was much higher in smooth muscle cells and clearly suppressed in the presence of formoterol (Figs. 2 and 3). Measurements of Ca^{2+} time-courses in buffer media containing either 1.3 mM $CaCl_2$ or 1 mM EGTA demonstrated that both the intracellular release of Ca^{2+} and the overall influx through the plasma membrane were strongly antagonized by pretreatment of the cells with 50 nM formoterol. The hormone-induced rapid rise in cytosolic Ca^{2+} was primarily of transient nature in all cell fractions. Sequestration of Ca^{2+} back to intracellular storage sites and Ca^{2+} efflux *via* the membrane-bound Ca^{2+} ATPase and the Na^+/Ca^{2+} exchanger are certainly the key elements responsible for the transient character of the angiotensin II-induced Ca^{2+} signal [66]. Strikingly, the elimination of Ca^{2+} ($1/\tau_{el}$) from the cytoplasm was clearly accelerated by pretreatment of the cells with formoterol and cytosolic Ca^{2+} concentration decreased almost to the starting value at a formoterol concentration of 50 nM (Table 1). Most likely, the activities of Ca^{2+} ATPase and the Na^+/Ca^{2+} exchanger were enhanced in formoterol-pretreated cells. Nevertheless, the exact mechanism by which formoterol catalyzed the elimination of Ca^{2+} from the cytoplasm still remains to be elucidated. Assuming a linear relationship between Ca^{2+} release and the decrease in cell diameter ($d = 2 \cdot r$), the excitation-contraction coupling was calculated to be more efficient in control cells by almost 20%. An increase in cytosolic Ca^{2+} of 134.0 nM caused a length contraction of 4.76 μm (gradient = 3.6 ($\pm$ 0.1) 10^{-2} μm/nM) in the control cell group, whereas a Ca^{2+} increase of 59.5 nM diminished the diameter in formoterol-pretreated cells by only 1.80 μm (gradient = 3.0 ($\pm$ 0.2) $\cdot 10^{-2}$ μm/nM). The cell radius of the formoterol cells at 160 nM (i.e., at the basal Ca^{2+} level of the control cells) was 14.91 μm. The slightly larger cell radius at 160 nM ($r_{control}$ = 14.82 μm) after pretreatment with formoterol, as well as the weaker excitation-contraction coupling, may be attributed to an enhanced phosphorylation of myosin light-chain kinase and to a cAMP-related generation of relaxant cGMP. In both cell groups, the covariance matrix indicated strong correlations between the various fitting constants in Eqn (6) and, in particular, between the two Ca^{2+} pathways. This observation is in excellent harmony with the view that $InsP_3$ and its phosphorylated product, $Ins(1,3,4,5)P_4$, act synergistically in enhancing the permeability of the plasma membrane towards Ca^{2+} [67].

In the continuous presence of a receptor agonist such as angiotensin II, myosin light-chain phosphorylation is transient, although a constant level of isometric force is maintained. Recent results suggest that cAMP impairs the activity of kinases, which are related to the protein kinase C branch of the Ca^{2+} messenger system and activate a phosphoprotein phosphatase that catalyzes the dephosphorylation of a number of the late-phase proteins involved in sustaining the contractile reaction [55]. However, further Ca^{2+}-dependent regulatory events have been associated with the tonic phase of contraction. Rasmussen *et al.* [68] proposed that PKC-mediated phosphorylation of structural and regulatory components of the filamin-actin-desmin fibrillar domain may be responsible for sustained smooth

muscle contraction. In agreement with these results, Troyer *et al.* reported [69] that phorbol esters cause a slow and persistent contraction of mesangial cells, a specialized type of vascular smooth muscle cell [43, 44]. Much to our surprise, the contractile response of mesangial cells to a challenge with angiotensin II was potentiated in PKC-depleted cells as compared to control cells [20], suggesting that Ca^{2+} is the major determinant of angiotensin II-induced cell contraction. The contribution of PKC is an inhibitory one, leading to a rapid desensitization of hormone-stimulated signaling events. Recently, it has been reported that a hormone-stimulated K^+ depolarization of smooth muscle causes myosin light-chain phosphorylation at a specific position within the molecule, one sufficient for contraction [70, 71]. Because no phosphorylations at PKC sites were observed, these results strongly suggest that PKC plays no physiological role in maintaining tonic force by regulating the level of myosin light-chain phosphorylation.

The results of Murray implicate the release of Ca^{2+} from intracellular stores in the initiation of contraction, whereas the tonic (sustained) phase of contraction is associated with a Ca^{2+} influx through receptor-operated (ROCC) Ca^{2+} channels [39]. As far as smooth muscles are concerned, there is ample, convincing evidence that voltage-operated (VOCC) and receptor-operated (ROCC) Ca^{2+} channels are present [65]. Interestingly, drugs that block calcium entry through VOCC, such as nifedipine, verapamil, and diltiazem, have not proved effective in asthma [72], a result suggesting that Ca^{2+} entry *via* VOCC is of minor importance in human airway smooth muscle contractions.

Measurements in the presence and absence of 1.3 mM $CaCl_2$ in the buffer solution (data not shown) revealed that the transient component of angiotensin II-induced smooth muscle contraction could be attributed in both cell fractions to a release of Ca^{2+} from intracellular sources. However, whereas the control cells remained in a contracted state and relaxed only partially following a challenge with angiotensin II, the contractile response of formoterol-pretreated cells was transient in character. Noticeably, the cytosolic Ca^{2+} level persistently stabilized on a higher plateau in the control cell group (C_2/response = 11%) after simulation with angiotensin II, and cytosolic Ca^{2+} concentration decreased almost to the starting value in formoterol-pretreated cells (Table 1). Nevertheless, the cytosolic Ca^{2+} level in smooth muscle cells only remained elevated over a long time period (>30 min) if the buffer medium contained Ca^{2+}. Upon complexation of Ca^{2+} with EGTA, the angiotensin II-induced Ca^{2+} signal was purely transient even in control cells, and their cell volume relaxed to the initial value. Obviously, the calcium ions leading to a sustained elevation in cytosolic Ca^{2+} come from the extracellular fluid rather than from internal reservoirs. All these results strongly support Murray's hypothesis that the tonic phase of contraction is maintained by an influx of Ca^{2+} through ROCCs. Moreover, the amount (C_2) and the rate ($1/\tau_{in2}$) of Ca^{2+} influx, as well as the strength of the sustained contraction, were decreased continuously by incubating the cells with increasing formoterol concentrations. After pretreatment with 50 nM formoterol, the net influx of Ca^{2+} was almost completely abolished and the tonic phase of contraction was essentially missing. Murray's model is further supported by the observation that the time-constants τ_{rel}, which characterize the relaxation of the transient phase of contraction, closely match the decay times τ_{el} attributed to the transient Ca^{2+} signal. Furthermore, the parameters τ_{c2} (defining the time progression of the sustained contraction) were within the experimental error identical to the Ca^{2+} influx time constants τ_{in2}.

Nevertheless, the limitation of Murray's model should be clearly recognized. As has been demonstrated by Ochsner *et al.* [20], a long-term pretreatment of mesangial cells with human interleukin-1β (1 nM, 24 hr) increased the angiotensin II-induced mobilization of Ca^{2+} from intra- and extracellular sources, but simultaneously reduced the contractile responses of the transient and tonic phases. The data could be satisfactorily explained by an IL-1β-dependent rise in intracellular nitric oxide concentration that activated soluble guanylate cyclase and led to an increase in cGMP, a species known to induce an immediate relaxation of contracted cells [43, 44]. Consequently, the stimulation of smooth muscle cells with a substrate that acts synergistically with cAMP to enhance the generation of cGMP may invalidate Murray's model by strongly counteracting Ca^{2+}-induced contraction.

Altogether, the β_2-adrenergic receptor is linked to the ultimate cellular response (i.e., muscle relaxation) by a transduction mechanism that consists of a stimulatory G protein (G_s) and the catalytic subunit of adenylate cyclase. The interaction has been termed 'collision coupling' and has been found to be enhanced when the microviscosity of the cell membrane is lowered [40, 50, 73]. As demonstrated by Stubbs and Smith [73], a decrease in microviscosity mostly leads to substantial changes in the local organization within the plasmalemma (e.g., lateral phase separations) and potentiates the generation of cAMP by a higher mobility and activity of adenylate cyclase. The ring of lipids immediately surrounding adenylate cyclase acts to solvate the membrane protein into the lipid bilayer. The physical properties of the cell membrane, in particular its fluidity or rigidity, not only influence the lateral migration of the activating $\alpha_s \cdot$ GTP component, but also the internal motions of groups and peptide chains connected to the function of adenylate cyclase [50]. This explains the high sensitivity of the enzyme activity to minor changes in its environment.

For lipophilic drugs such as formoterol, the partition equilibrium is very much in favor of the plasmalemma lipid bilayer. The intercalation of formoterol into cell membranes lowers their microviscosity and, consequently, leads to a stronger coupling between the β_2-adrenoceptor glycoprotein and adenylate cyclase [40]. The activities of phos-

pholipase C, PKA, and myosin light-chain kinase are also expected to be enhanced due to the higher fluidity of the hydrophobic environment in muscle fibers. As shown in Table 3, the initiation of the contractile response subsequent to the intracellular release of Ca^{2+} was delayed in the control cell group compared to cells pretreated with formoterol. The β_2-adrenoceptor agonist formoterol obviously causes a faster transduction of the angiotensin II-mediated signal to the contractile elements of the cell. Consistent with the idea of an accelerated transmission of angiotensin II-dependent processes, the rate ($1/\tau_{in1}$) representing $InsP_3$-induced Ca^{2+} release from internal stores also tended to be somewhat larger in formoterol-pretreated cells. In contrast to this, the speed of contraction (characterized by the variables $[dV/dt]_{max}$ and $1/\tau_{c1}$) was slower after a pretreatment with formoterol, probably through the antagonizing effect of cAMP-mediated processes or through the inhibitory influence of formoterol-associated hyperpolarization on contractile response.

The results obtained are in excellent agreement with those of Anderson *et al.* [12]. The lipid bilayer of airway smooth muscle acts as a depot for formoterol and explains its long-acting antiasthmatic effect. As compared to the more lipophilic β_2-adrenoceptor agonist salmeterol ($\log_{10}(K_{pmem})$ = 4.22 ± 0.01; pH = 7.0; 20°C) [42], there are, however, sufficient formoterol molecules available in the aqueous biophase to permit an immediate interaction with the active site of the β_2-adrenergic receptor. The low microviscosity of the plasma membrane enables a rapid lateral diffusion of formoterol to the active site of the β_2-adrenoceptor, which is composed of seven transmembrane spanning protein sequences arranged in α-helices [74, 75]. Remarkably, the presence of lipophilic substituents at the benzene rings leads to a higher β_2/β_1-selectivity; thus, minimizing cardiovascular side effects (tachycardias, arrhythmias, and extrasystoles, etc.) [76]. As shown by El Tayar *et al.*, β_2-selectivity increases linearly with the logarithm of the *n*-octanol/water partition coefficient [$\log_{10}(P_{ow})$] measured at pH = 7.4 [76]. In addition, the binding of a β_2-agonist to its correspondent receptor in lung tissue is highly stereoselective [76]. Notably, Ciba-Geigy's formoterol consists of an exact 1:1 mixture of the (R;R) and (S;S) enantiomers, where the potency of the (R;R) form has been shown to be higher by a factor of *ca.* 1000 [77].

Even though radioligand studies indicated [36] that the density of β_2-adrenoceptors was identical in both cell fractions, the persistent use of β_2-stimulating agents often leads to tachyphylaxis. Studies performed on cellular models have shown that the observed effects are initiated by phosphorylations of β_2-adrenoceptor glycoproteins through cAMP-dependent and -independent protein kinases [78]. These modifications of the β_2-receptor ultimately lead to a decrease in the density of β_2-adrenoceptors (downregulation) on airway smooth muscle and on inflammatory cells by incorporation of phosphorylated β_2-adrenoceptor glycoproteins into cytoplasmic vesicles [78].

CONCLUSIONS

From the results obtained, we conclude that the protective effect of formoterol on bronchospasm is primarily mediated by an enhanced generation of cAMP. Like all β_2-adrenoceptor agonists, formoterol strongly activates adenylate cyclase through a stimulatory guanyl nucleotide binding protein (G_s). However, because the drug rapidly partitions into the acyl side chain region of the lipid bilayers and increases the fluidity of the plasma membrane, coupling between the β_2-adrenoceptor glycoprotein and the associated adenylate cyclase is intensified and the production of cAMP drastically enhanced. The elevated cAMP level in formoterol-pretreated cells ultimately leads to a reduced phosphorylation of myosin and, consequently, to a decreased coupling between the actin and myosin components. Moreover, cAMP suppresses angiotensin II-induced cell contraction by restraining phosphoinositide breakdown and impairing excitation-contraction coupling, possibly through an activation of the protein kinase C pathway. In addition, pretreatment with formoterol leads to a hyperpolarization of the resting membrane potential, considered the dominant electrophysiological effect of β_2-adrenergic drugs. The formoterol-associated hyperpolarization of the plasma membrane additionally contributes to counteract the increase in cytosolic Ca^{2+} and to attenuate the contractile response of smooth muscle cells.

Despite the widespread distribution of β_2-adrenoceptors in lung tissue, β_2-agonists reverse airway obstruction primarily by relaxing airway smooth muscle. As outlined above, various inflammatory mediators have been implicated in the pathogenesis of asthma [5]. All these substances are synthesized and released by mast cells and polymorphonuclear leukocytes after challenge with their specific antigen. When inhaled prior to allergen challenge, β_2-adrenoceptor agonists are powerful mast cell stabilizing drugs, both *in vitro* and *in vivo* [79]. The adenylate cyclase-related increase in cAMP concentration inhibits a rapid release of inflammatory mediators and protects lung smooth muscle from acute bronchoconstrictions [80]. However, long-acting β_2-adrenergic agonists, such as formoterol or salmeterol, are significantly more powerful in suppressing late asthmatic bronchoconstriction that reaches its maximum 6–8 hr after challenge and lasts for up to 24 hr [81]. Whereas classic β_2-adrenoceptor agonists appear to be ineffective in controlling airway inflammation and mucus production in asthmatics, it is, at the time of the writing of this paper, not yet clear whether or not the attenuation of late-phase reactions by long-acting β_2-adrenoceptor agonists can be attributed to an anti-inflammatory action of these drugs.

Notwithstanding, the powerful action of bronchodilators may mask the onset and/or exacerbation of airway inflammation in asthma patients, resulting in the underutilization of effective inflammatory agents. The primary therapy should, therefore, focus on treatment of the inflammation.

An adequate use of long-acting β_2-adrenoceptor agonists, such as formoterol or salmeterol, is certainly beneficial by producing bronchodilatation and, possibly, curative by suppressing the inflammatory process.

Thanks are due to Prof. J. Pfeilschifter and G. Walker for the cultivation of smooth muscle cells and to G. P. Anderson for helpful discussions. The publication of this manuscript was supported by a grant from the "Schweizerische Krebsliga."

References

1. Paterson JW, Woolcock AJ and Shenfield GM, Bronchodilator drugs. *Am Rev Respir Dis* **120:** 1149–1188, 1979.
2. Behrman RE and Vaughan VC, Asthma. In: *Nelson Textbook of Pediatrics* (Ed. Nelson WE), 13th ed., pp. 495–501. WB Saunders Company, Philadelphia, 1987.
3. Chanez P, Bousquet J and Michel FB, The pathogenesis of asthma. *Odyssey* **1:** 24–33, 1994.
4. Reed CE, New therapeutic approaches in asthma. *J Allergy Clin Immunol* **77:** 537–543, 1986.
5. von Sprecher A, Beck A, Sallmann A, Breitenstein W, Wiestner H, Kimmel S, Anderson GP, Subramanian N and Bray MA, Peptidoleukotriene antagonists: Structural analogs of leukotriene D4 with special emphasis on CGP 45715A. *Drugs Future* **16:** 827–843, 1991.
6. Page CP and Barnes PJ, *Pharmacology of Asthma* (Eds.), Springer-Verlag, New York, 1991.
7. Chung KF and Barnes PJ, Role of inflammatory mediators in asthma. *Br Med Bull* **48:** 135–148, 1992.
8. Barnes PJ, New therapeutic approaches. *Br Med Bull* **48:** 231–247, 1992.
9. National Heart, Lung and Blood Institute, *International consensus report on diagnosis and management of asthma.* (NIH publication No. 91-3091) National Institutes of Health, Bethesda, MD, 1992.
10. Barnes PJ, Effect of corticosteroids on airway hyperresponsiveness. *Am Rev Respir Dis* **137:** S70–S76, 1990.
11. Drazen JM and Israel E, Treating mild asthma—when are inhaled steroids indicated? *N Engl J Med* **331:** 737–739, 1994.
12. Anderson GP, Lindén A and Rabe KF, Why are long-acting beta-adrenoceptor agonists long-acting? *Eur Respir J* **7:** 569–578, 1994.
13. Naline E, Zhang Y, Qian Y, Mairon N, Anderson GP, Grandordy B and Advenier C, Relaxant effects and durations of action of formoterol and salmeterol on the isolated human bronchus. *Eur Respir J* **7:** 914–920, 1994.
14. Becker AB, Simons FER, McMillan JL and Faridy T, Formoterol, a new long-acting selective β_2-adrenergic receptor agonist: double-blind comparison with salbutamol and placebo in children with asthma. *J Allergy Clin Immunol* **84:** 891–895, 1989.
15. Ullman A and Svedmyr N, Salmeterol, a new long acting inhaled β_2-adrenoceptor agonist: comparison with salbutamol in adult asthmatic patients. *Thorax* **43:** 674–678, 1988.
16. Pearce N, Beasley R, Crane J, Burgess C and Jackson R, End of New Zealand asthma mortality epidemic. *Lancet* **345:** 41–44, 1995.
17. Sly RM, Anderson JA and Bierman CW, Adverse effects and complications of treatment with beta-adrenergic agonist drugs. *J Allergy Clin Immunol* **75:** 443–449, 1985.
18. Molfino NA and Slutsky AS, Near fatal asthma. *Eur Resp J* **7:** 981–990, 1994.
19. Fandrey J and Jelkmann W, Prostaglandin E_2 and atriopeptin III oppose the contractile effect of angiotensin II in rat kidney mesangial cell cultures. *Prostaglandines* **36:** 249–257, 1988.
20. Ochsner M, Fleck T, Kernen P, Deranleau DA and Pfeilschifter J, Simultaneous registration of Ca^{2+} transients and volume changes in rat mesangial cells—Evaluation of the effects of protein kinase C down-regulation. *J Fluorescence* **2:** 37–45, 1992.
21. Pfeilschifter J and Rüegg UT, Cyclosporin A augments angiotensin II-stimulated rise in intracellular free calcium in vascular smooth muscle cells. *Biochem J* **248:** 883–887, 1987.
22. Pfeilschifter J, Ochsner M, Whitebread S and De Gasparo M, Down-regulation of protein kinase C potentiates angiotensin II-stimulated polyphosphoinositide hydrolysis in vascular smooth muscle cells. *Biochem J* **262:** 285–291, 1989.
23. Kreisberg JI, Venkatachalam MA, Radnik RA and Patel PY, Role of myosin light-chain phosphorylation and microtubules in stress fiber morphology in cultured mesangial cells. *Am J Physiol* **249:** F227–F235, 1985.
24. Travo P, Weber K and Osborn M, Co-existence of vimentin and desmin type intermediate filaments in a subpopulation of adult rat vascular smooth muscle cells growing in primary culture. *Exp Cell Res* **139:** 87–94, 1982.
25. Tsien R and Pozzan T, Measurement of cytosolic free Ca^{2+} with quin2. In: *Methods in Enzymology* **172:** (Eds. Fleischer S and Fleischer B), pp. 230–262. Academic Press, New York, 1989.
26. Grynkiewicz G, Poenie M, Tsien RY, A new generation of Ca^{2+} indicators with greatly improved fluorescence properties. *J Biol Chem* **260:** 3440–3450, 1985.
27. Minta A, Kao JP, and Tsien RY, Fluorescent indicators for cytosolic calcium based on rhodamine and fluorescein chromophores. *J Biol Chem* **264:** 8171–8178, 1989.
28. Ochsner-Bruderer M and Fleck T, Anmerkungen zur fluorimetrischen Bestimmung der intrazellulären Calciumionenkonzentration. *Nachr Chem Tech Lab* **41:** 997–1002, 1993.
29. van de Hulst HC, *Light scattering by Small Particles*. Wiley & Sons, New York, 1957.
30. Bolin FP, Preuss LE, Taylor RC and Ference RJ, Refractive index of some mammalian tissues using a fiber optic cladding method. *Appl Opt* **28:** 2297–2303, 1989.
31. Lakowicz JR, *Principles of Fluorescence Spectroscopy*. Plenum Press, New York, 1983.
32. Kuhry J-G, Duportail G, Bronner C and Laustriat G. Plasma membrane fluidity measurements on whole living cells by fluorescence anisotropy of trimethylammoniumdiphenylhexatriene. *Biochem Biophys Acta* **845:** 60–67, 1985.
33. Lakowicz JR and Prendergast FG, Detection of hindered rotations of 1,6-diphenyl-1,3,5-hexatriene in lipid bilayers by differential polarized phase fluorometry. *Biophys J* **24:** 213–231, 1978.
34. Pfeilschifter J, Fandrey J, Ochsner M, Whitebread S and De Gasparo M, Potentiation of angiotensin II-stimulated phosphoinositide hydrolysis, calcium mobilization and contraction of renal mesangial cells upon down-regulation of protein kinase C. *FEBS Lett* **261:** 307–311, 1990.
35. Ochsner M, Creba J, Walker J, Bentley P and Muakkassah-Kelly SF, Nafenopin, a hypolipidemic and non-genotoxic hepatocarcinogen increases intracellular calcium and transiently decreases intracellular pH in hepatocytes without generation of inositol phosphates. *Biochem Pharmacol* **40:** 2247–2257, 1990.
36. Ochsner M and Kunz D, unpublished results, 1994.
37. Hecht E, *Optics*. 2nd ed., pp. 170. Addison-Wesley Publishing Company, Reading, MA, 1987.
38. Tsien RY, Pozzan T and Rink TJ, Calcium homeostasis in intact lymphocytes: cytoplasmic free calcium monitored with a new, intracellularly trapped fluorescent indicator. *J Cell Biol* **94:** 325–334, 1982.
39. Murray RK and Kotlikoff MI, Receptor-activated calcium influx in human airway smooth muscle cells. *J Physiol* **435:** 123–144, 1991.

40. Houslay MD and Gordon LM, The activity of adenylate cyclase is regulated by the nature of its lipid environment. *Current Topics Membranes Transp* **18:** 179–231, 1983.
41. Höer A and Oberdisse E, Das Phosphoinositid-Phospholipase-C-System. *Med Mo Pharm* **13:** 243–252, 1990.
42. John E, Ochsner M, Jaekel K, Mutz M and Anderson GP, Comparative biophysical analysis of interactions between bronchodilator drugs with lipid membranes (to be submitted for publication).
43. Pfeilschifter J, Regulatory functions of protein kinase C in glomerular mesangial cells. *Klin Wochenschr* **68:** 1134–1137, 1990.
44. Pfeilschifter J, Cross-talk between transmembrane signalling systems: a prerequisite for the delicate regulation of glomerular haemodynamics by mesangial cells. *Eur J Clin Invest* **19:** 347–361, 1989.
45. Anand-Srivastava MB, Enhanced expression of inhibitory guanine nucleotide regulatory protein in spontaneously hypertensive rats. Relationship to adenylate cyclase. *Biochem J* **288:** 79–85, 1992.
46. Barnes PJ, Neural control of human airways in health and disease. *Am Rev Respir Dis* **134:** 1289–1314, 1986.
47. Silver PJ and Stull JT, Regulation of myosin light chain and phosphorylase phosphorylation in tracheal smooth muscle. *J Biol Chem* **257:** 6145–6150, 1982.
48. Linder ME and Gilman AG, G proteins. *Scientific American* **267**(1): 36–43, 1992.
49. Stryer L, *Biochemistry*. 3rd ed. WH Freeman and Company, New York, 1988.
50. Houslay MD and Stanley KK, *Dynamics of Biological Membranes: Influence on Synthesis, Structure and Function*. Wiley & Sons, New York, 1982.
51. Lulich KM, Goldie RG and Paterson JW, β-adrenoceptor function in asthmatic bronchial smooth muscle. *Gen Pharmacol* **19:** 307–311, 1988.
52. Kamm KE and Stull JT, The function of myosin and myosin light chain kinase phosphorylation in smooth muscle cells. *Annu Rev Pharmacol Toxicol* **25:** 593–620, 1985.
53. Morley J, *Perspectives in Asthma 2: β-adrenoceptors in Asthma* (Ed.), Academic Press, London, 1984.
54. Ito Y and Itoh T, Effects of isoprenaline on the contraction-relaxation cycle in the cat trachea. *Br J Pharmacol* **83:** 677–686, 1984.
55. Rasmussen H, Kelley G and Douglas JS, Interactions between Ca^{2+} and cAMP messenger system in regulation of airway smooth muscle contraction. *Am J Physiol* **258:** L279–L288, 1990.
56. Imai T, Hirata Y, Kanno K and Marumo F, Induction of nitric oxide synthase by cyclic AMP in rat vascular smooth muscle cells. *J Clin Invest* **93:** 543–449, 1994.
57. Lugnier C, Calcium-calmoduline et vasomotricite. *Arch Mal Coeur Vaiss* **84:** 25–34, 1991.
58. Bredt DS and Snyder SH, Nitric Oxide: A physiologic messenger molecule. *Annu Rev Biochem* **63:** 175–195, 1994.
59. Nakashima M, Vanhoutte PM, Isoproterenol causes hyperpolarization through opening of ATP-sensitive potassium channels in vascular smooth muscle of the canine saphenous vein. *J Pharmacol Exp Ther* **272:** 379–384, 1995.
60. Kume H, Hall IP, Washabau RJ, Takagi K and Kotlikoff I, β-adrenergic agonists regulate KCa channels in airway smooth muscle by cAMP-dependent and -independent mechanisms. *J Clin Invest* **93:** 371–379, 1994.
61. Scheid CR, Honeyman TW and Fay FS, Mechanism of β-adrenergic relaxation of smooth muscle. *Nature* **277:** 32–36, 1979.
62. Knox AJ and Brown JK, Differential regulation of Na/K ATPase by the cyclic nucleotide dependent protein kinases in airway smooth muscle. *Clin Res* **39:** 331A, 1991.
63. Ochsner M, unpublished results, 1995.
64. Ochsner M, Fleck T and Waldmeier P, Simultaneous measurement of Ca^{2+} transients and of membrane depolarizations in synaptosomes. *Biochem Biophys Res Comm* **181:** 797–803, 1991.
65. Rodger IW, Airway smooth muscle. *Br Med Bull* **48:** 97–107, 1992.
66. Carafoli E, Intracellular calcium homeostasis. *Ann Rev Biochem* **56:** 395–433, 1987.
67. Berridge MJ and Irvine RF, Inositol phosphates and cell signalling. *Nature* **341:** 197–205, 1989.
68. Rasmussen H, Takuwa Y and Park S, Protein kinase C in the regulation of smooth muscle contraction. *FASEB J* **1:** 177–185, 1987.
69. Troyer DA, Gonzalez OF, Douglas JG and Kreisberg JI, Phorbol ester inhibits arginine vasopressin activation of phospholipase C and promotes contraction of, and prostaglandin production by, cultured mesangial cells. *Biochem J* **251:** 907–912, 1988.
70. Kamm KE, Hsu LC, Kubota Y and Stull JT, Phosphorylation of smooth muscle myosin heavy and light chains. Effect of phorbol dibutyrate and agonists. *J Biol Chem* **264:** 21223–21229, 1989.
71. Singer HA, Oren JW and Benscoter HA, Myosin light chain phosphorylation in ^{32}P-labeled rabbit aorta stimulated by phorbol 12,13-dibutyrate and phenylephrine. *J Biol Chem* **264:** 21215–21222, 1989.
72. Barnes PJ, Clinical studies with calcium antagonists in asthma. *Br J Clin Pharmacol* **20:** S289–S298, 1985.
73. Stubbs CD and Smith AD, The modification of mammalian membrane polyunsaturated fatty acid composition in relation to membrane fluidity and function. *Biochim Biophys Acta* **779:** 89–137, 1984.
74. Fraser CM and Venter JC, Beta-adrenergic receptors. Relationship of primary structure, receptor function and regulation. *Am Rev Respir Dis* **141:** S22–S30, 1990.
75. Cronet P, Sander C and Vriend G, Modeling of transmembrane seven helix bundles. *Protein Eng* **6:** 59–64, 1993.
76. El Tayar N, Testa B, van de Waterbeemd H, Carrupt P-A and Kaumann AJ, Influence of lipophilicity and chirality on the selectivity of ligands for β_1- and β_2-adrenoceptors. *J Pharm Pharmacol* **40:** 609–612, 1988.
77. Trofast J, Osterberg K, Kallstrom BL and Waldeck B, Steric aspects of agonism and antagonism at beta-adrenoceptors: synthesis of and pharmacological experiments with the enantiomers of formoterol and their diastereomers. *Chirality* **3:** 443–450, 1991.
78. Cros G, Mécanismes de la désensibilisation des récepteurs beta-adrenergiques. *Bull Eur Physiopathol Respir* **21**(5): S35–S43, 1985.
79. Church MK and Hiroi J, Inhibition of IgE-dependent histamine release from human dispersed lung mast cells by anti-allergic drugs and salbutamol. *Br J Pharmacol* **90:** 421–429, 1987.
80. Soll AH and Toomey M, Beta-adrenergic and prostanoid inhibition of canine fundic mucosal mast cells. *Am J Physiol* **256:** G727–G732, 1989.
81. Palmqvist M, Balder B, Lowhagen O, Melander B, Svedmyr N and Wahlander L, Late asthmatic reaction decreased after pretreatment with salbutamol and formoterol, a new long-acting beta 2-agonist. *J Allergy Clin Immunol* **89:** 844–849, 1992.